

Morphological stability of a two-dimensional cylindrical crystal with a square-law supersaturation dependence of the growth rate

This article has been downloaded from IOPscience. Please scroll down to see the full text article.

2005 J. Phys.: Condens. Matter 17 2889

(<http://iopscience.iop.org/0953-8984/17/19/006>)

View [the table of contents for this issue](#), or go to the [journal homepage](#) for more

Download details:

IP Address: 129.252.86.83

The article was downloaded on 27/05/2010 at 20:43

Please note that [terms and conditions apply](#).

Morphological stability of a two-dimensional cylindrical crystal with a square-law supersaturation dependence of the growth rate

L M Martyshev and E A Chervontseva

Institute of Industrial Ecology, Russian Academy of Sciences, S Kovalevskaya Street 20A, Ekaterinburg 620219, Russia

E-mail: mlm@ecko.uran.ru

Received 3 November 2004, in final form 30 March 2005

Published 29 April 2005

Online at stacks.iop.org/JPhysCM/17/2889

Abstract

The morphological stability of a two-dimensional cylindrical crystal growing in a solution at the local growth rate proportional to the squared supersaturation has been analysed for the first time by the weakly nonlinear technique. A correction to the stability size, which was determined from the linear stability theory, was found and analysed. It was shown that in most cases the critical size of the crystal stability decreased with growing perturbation amplitude. This result has been discussed in terms of the nonequilibrium phase transition theory.

1. Introduction

Factors responsible for the appearance of complicated three-dimensional structures cannot be understood if one does not analyse the initial stage when a growing crystal loses its morphological stability. It is this stage that largely determines the subsequent shape of the crystal and lends itself to relatively rigorous calculations in analytical terms. Although the appearance and the evolution of an instability on the crystal surface have been studied intensively [1], many problems, which present interest from both practical and theoretical viewpoints, are still not clearly understood [2, 3]. We shall mention two of them, which are directly related to the present study.

(1) The morphological stability of a growing crystal is traditionally analysed using the theory of perturbations for solving problems concerned with heat and mass transfers on a moving boundary [1]. The available experimental studies of the morphological stability of a growing crystal provide a qualitative support to many inferences that follow from this theory (for example, the dependence of the size of the crystal stability on the supersaturation/supercooling, surface properties, the presence of convection, etc). However, it should be acknowledged that the theory of the stability of freely growing crystals has not so far been put to a systematic quantitative verification, although it has been developing for over

40 years. One of the reasons is the numerous simplifications, which are necessarily introduced in theoretical calculations even when the initial stage of the instability is concerned. As a result, the natural aspiration to better clarity and simplicity of the final formulae makes the correct experimental verification impossible because these simplifications are difficult (and, sometimes, impossible) to realize in experiments. For example, the behaviour of the crystal boundary in the presence of perturbations having infinitesimal amplitudes has been analysed theoretically in sufficient detail (the linear analysis) [1]. However, problems of the shape perturbation with harmonics of a small, but finite, amplitude (the weakly nonlinear analysis) have received very little study [4–7], although they present the greatest practical significance¹ and are much easier to analyse experimentally. This is because these problems are tedious and complicated. The weakly nonlinear analysis was performed earlier only with respect to the free growth of the crystal nuclei having a simple (spherical or cylindrical) geometry on the assumption of infinitely fast kinetic processes on the surface (the so-called diffusion limited regime) [4–6]. It was found that the critical stability size of crystals decreases virtually at all times as the perturbation is enhanced. This is probably an indication that these morphological transformations are first-order nonequilibrium phase transitions [2, 3, 8]. However, a considerable limitation of the aforementioned studies is the assumption on a diffusion mechanism of the growth, i.e. the surface kinetics was disregarded altogether, although it has a very large effect on the morphological stability [1, 9, 10]. It is known that surface processes are quite different on atomically smooth and rough surfaces. In the case of rough surfaces, which have a lot of favourable sites for the attachment of atoms, the local growth rate of a crystal proves to be proportional to the supersaturation (supercooling) at the crystallization front. The experimental and theoretical studies demonstrated that this dependence is observed for the growth from some melts (e.g., cyclohexanol, succinonitrile, Fe, Ni) [11] and, occasionally, from solutions (e.g., crystallization of NH_4Cl from water) [10]. In our later study [7] we made calculations on the assumption that the local growth rate of the crystal was proportional to the supersaturation. These calculations provided original data concerning the behaviour of the critical stability radius depending on the perturbation frequency and amplitude under intermediate and kinetic regimes of the crystal growth. One more issue, which is significant for both practical applications and the quantitative experimental verification of the theory of the morphological stability, is calculations of the stability of crystals with atomically smooth surfaces. In this case, the kinetics of surface processes is determined not only by elementary exchange events on surface steps, but also by their density. The number of surface steps depends on the capacity of step generators (dislocations and nuclei), which considerably changes with the supersaturation. Therefore, the supersaturation (supercooling) dependence of the growth rate is nonlinear and is nearly quadratic for smooth surfaces [9, 10]. Although this dependence is observed for the growth of crystals from the majority of solutions and vapours and, also, from some melts, the weakly nonlinear analysis for the morphological stability has not been performed so far. The reason is largely cumbersome calculations involved in this considerably nonlinear problem.

(2) The much used linear analysis for the morphological stability does not explain one feature, which is observed during the nonequilibrium growth of crystals. It turns out that the crystallization control parameters (for example, supercooling) have a region of values when crystals of different shapes may appear simultaneously [2, 3, 12–14]. The so-called coexistence of different morphological phases takes place [2, 3]. In this case, morphologically different crystals may develop simultaneously both from different nuclei [12] and from one seed [14].

¹ These studies allow, in particular, for understanding how various (acoustic, thermal, electromagnetic, etc) effects and different inhomogeneities near the surface (impurities, air bubbles, etc) affect the morphology (and, hence, crystal properties).

A relatively close similarity is noted in the literature concerning classical equilibrium phase transitions and transitions from one nonequilibrium growth form to another [2, 3]. It is known that ordinary phase transitions are also accompanied by the coexistence of phases over the so-called metastable interval. Let us consider a characteristic example, namely the solidification of water. It is known that water can be supercooled to 40° below its traditional solidification point of 273 K depending on the presence of various perturbations (impurities, etc) [10]. As a result, both phases of water (ice and liquid) can be observed at temperatures from 233 to 273 K depending on crystallization conditions. Let us emphasize that the more accurate are the experimental conditions (smoother walls of the crystallization vessels, the absence of foreign microscopic particles, etc), the stronger the supercooling of water can be. Correspondingly, the fewer the precautions that are taken in the experiment (the greater the number of various perturbations), the earlier the water will crystallize. It would be interesting to see if this regularity holds for morphological transformations. One of the possible theoretical methods of verification² is just the weakly nonlinear analysis for the morphological stability, which gives an explicit dependence of the transition point (the so-called critical size (radius) of the stability) on the perturbation amplitude. Obviously, if it is found that the crystal stability size decreases with growing perturbation, these calculations will give an insight into the phenomenon of the coexistence of morphological phases.

Considering the above-adduced arguments, the weakly nonlinear analysis of the morphological stability of a freely growing crystal at a quadratic dependence of the local growth rate on the supersaturation seems to be very important and interesting today. This is the subject matter of the present study.

2. Problem statement

The mathematical model is constructed as follows. Let us consider a two-dimensional quasi-steady-state growth of an initially round single crystal in a supersaturated solution under isothermal and isobaric conditions. The concentration field C is given by the Laplace equation

$$\nabla^2 C = 0, \quad (1)$$

where ∇^2 is the Laplacian operator. The following boundary conditions are used:

$$C(R_\lambda) = C_\infty, \quad (2)$$

$$D \frac{\partial C}{\partial \tilde{\mathbf{n}}}\bigg|_{\tilde{r}_S} = \beta(C|_{\tilde{r}_S} - C_S)^2, \quad (3)$$

$$C_S = C_0 + C_0 \Gamma \tilde{K}, \quad (4)$$

$$\tilde{K} = \frac{\tilde{r}_S^2 + 2(\partial \tilde{r}_S / \partial \varphi)^2 - \tilde{r}_S \partial^2 \tilde{r}_S / \partial \varphi^2}{(\tilde{r}_S^2 + (\partial \tilde{r}_S / \partial \varphi)^2)^{3/2}},$$

where $\tilde{r}_S(\varphi, t) = R + a(t) \cos k\varphi$ is the equation for a perturbed boundary; $a(t)$ is the perturbation amplitude, ($a \ll R$); t is the time, $\tilde{\mathbf{n}}$ is the surface normal, φ is the polar angle, k is a positive integer (perturbation frequency), D is the diffusivity; R is the radius of an unperturbed round crystal; β is the crystallization kinetic coefficient, which varies from 0 (in the kinetic limited growth regime) to ∞ (in the diffusion limited growth regime); C_∞ is the solution concentration at a distance R_λ from the crystal ($R_\lambda \gg R$); C_S is the solute equilibrium concentration near an arbitrary interface; C_0 is the solute equilibrium concentration

² For another method, in which the entropy production is calculated, refer to [3, 8, 15].

near a flat interface; Γ is the capillary constant, which is proportional to the surface tension coefficient [16]; \tilde{K} is the curvature of a distorted circle boundary.

These boundary conditions are typical enough for crystallization from solutions (see, for example [3, 7, 16]). A squared relationship of the local growth rate and the supersaturation is explicitly present in (3).

Let us convert to dimensionless variables in (1)–(4) for convenience of the analysis. We shall use the nucleation radius $R^* = C_0\Gamma/(C_\infty - C_0)$ [16] as the length scale. The concentration field is defined as $u = (C - C_0)/C_0$. In this case, the equations (1)–(3) are transformed to

$$\nabla^2 u = 0; \tag{5}$$

$$u(\rho_\lambda) = \Delta; \tag{6}$$

$$\alpha \Delta \left. \frac{\partial u}{\partial \mathbf{n}} \right|_{\rho+\delta \cos(k\varphi)} = (u|_{\rho+\delta \cos(k\varphi)} - u_S)^2; \quad u_S = K \Delta. \tag{7}$$

Here $n = \tilde{n}/R^*$, $r = \tilde{r}/R^*$, $\rho = R/R^*$, $\delta(t) = a(t)/R^*$ and $\Delta = (C_\infty - C_0)/C_0$ denote the dimensionless solution supersaturation; $K = \tilde{K}R^*$, $\rho_\lambda = R_\lambda/R^*$, and $\alpha = D/\beta\Gamma C_0$ ($\alpha \rightarrow 0$ and $\alpha \rightarrow \infty$ in the diffusion and kinetic growth regimes respectively).

By analogy with [7], we write $\frac{\partial}{\partial \mathbf{n}}$ in (7) through components as

$$\frac{\alpha \Delta \left(\frac{\partial u}{\partial r} + \frac{\delta k}{r^2} \sin k\varphi \frac{\partial u}{\partial \varphi} \right)}{\sqrt{1 + \frac{\delta^2 k^2}{r^2} \sin^2 k\varphi}} \Big|_{\rho+\delta \cos(k\varphi)} = (u|_{\rho+\delta \cos(k\varphi)} - u_S)^2. \tag{8}$$

3. Weakly nonlinear analysis of the morphological stability

3.1. Calculation of the concentration field

Let us present the concentration field as a series in δ :

$$u(r, \varphi) = u_0(r) + u_1(r, \varphi)\delta + u_2(r, \varphi)\delta^2 + u_3(r, \varphi)\delta^3, \tag{9}$$

where u_0, \dots, u_3 denote expansion coefficients.

Substituting (9) into the initial equation (5) and the boundary conditions (6) and (8), we shall expand each term in a Taylor series about ρ to the third order in a small parameter δ .

In this case, the curvature is

$$K = K_0 + K_1\delta + K_2\delta^2 + K_3\delta^3, \tag{10}$$

where K_0, K_1, K_2 , and K_3 are given in the appendix. Equating the coefficients of the same order of δ on the opposite sides of each equation, we obtain four systems of equations for the determination of $u_0(r), u_1(r, \varphi), u_2(r, \varphi)$, and $u_3(r, \varphi)$:

$$\begin{aligned} \nabla^2 u_0 &= 0 \\ u_0(\rho_\lambda) &= \Delta \\ \alpha \Delta \left. \frac{\partial u_0}{\partial r} \right|_\rho &= (u_0|_\rho - K_0\Delta)^2 \end{aligned} \tag{11}$$

$$\begin{aligned} \nabla^2 u_1 &= 0 \\ u_1(\rho_\lambda) &= 0 \\ \alpha \Delta \left(\left. \frac{\partial^2 u_0}{\partial r^2} \right|_\rho \cos(k\varphi) + \left. \frac{\partial u_1}{\partial r} \right|_\rho \right) &= \left. \frac{\partial u_0^2}{\partial r} \right|_\rho \cos(k\varphi) + 2u_0|_\rho u_1|_\rho \\ &+ 2\Delta \left(\left. \frac{\partial u_0}{\partial r} \right|_\rho K_0 \cos(k\varphi) + u_0|_\rho K_1 + u_1|_\rho K_0 \right) - 2\Delta^2 K_0 K_1 \end{aligned} \tag{12}$$

$$\begin{aligned}
\nabla^2 u_2 &= 0 \\
u_2(\rho_\lambda) &= 0 \\
\alpha \Delta \left(\frac{1}{2} \frac{\partial^3 u_0}{\partial r^3} \Big|_\rho \cos^2(k\varphi) + \frac{\partial^2 u_1}{\partial r^2} \Big|_\rho \cos(k\varphi) \frac{k}{\rho^2} \frac{\partial u_1}{\partial \varphi} \Big|_\rho \sin(k\varphi) \right) \\
&= \frac{1}{2} \frac{\partial^2 u_0}{\partial r^2} \Big|_\rho \cos(k\varphi) + 2 \left(u_0|_\rho \frac{\partial u_1}{\partial r} \Big|_\rho + u_1|_\rho \frac{\partial u_0}{\partial r} \Big|_\rho \right) \cos(k\varphi) \\
&\quad + 2u_0|_\rho u_2|_\rho - 2\Delta \left[K_0 \left(\frac{1}{2} \frac{\partial^2 u_0}{\partial r^2} \Big|_\rho \cos^2(k\varphi) + \frac{\partial u_1}{\partial r} \Big|_\rho \cos(k\varphi) + u_2|_\rho \right) \right. \\
&\quad \left. + K_1 \left(\frac{\partial u_0}{\partial r} \Big|_\rho \cos(k\varphi) + u_1|_\rho \right) + K_2 u_0|_\rho \right] + \Delta^2 (K_1^2 + 2K_0 K_2) \quad (13)
\end{aligned}$$

$$\begin{aligned}
\nabla^2 u_3 &= 0 \\
u_3(\rho_\lambda) &= 0 \\
\alpha \Delta \left(\frac{1}{6} \frac{\partial^4 u_0}{\partial r^4} \Big|_\rho \cos^3(k\varphi) + \frac{1}{2} \frac{\partial^3 u_1}{\partial r^3} \Big|_\rho \cos^2(k\varphi) + \frac{k}{\rho^2} \frac{\partial}{\partial r} \left(\frac{\partial u_1}{\partial \varphi} \right) \Big|_\rho \sin(k\varphi) \cos(k\varphi) \right. \\
&\quad \left. - \frac{2}{\rho^3} \frac{\partial u_1}{\partial \varphi} \Big|_\rho \cos(k\varphi) + \frac{\partial^2 u_1}{\partial r^2} \Big|_\rho \cos(k\varphi) + \frac{k}{\rho^2} \frac{\partial u_1}{\partial r} \Big|_\rho \sin(k\varphi) + \frac{\partial u_3}{\partial r} \Big|_\rho \right) \\
&= \frac{1}{6} \frac{\partial^3 u_0}{\partial r^3} \Big|_\rho \cos^3(k\varphi) + 2 \left(\frac{1}{2} u_0|_\rho \frac{\partial^2 u_1}{\partial r^2} \Big|_\rho + \frac{\partial u_0}{\partial r} \Big|_\rho \frac{\partial u_1}{\partial r} \Big|_\rho \right. \\
&\quad \left. + \frac{1}{2} u_1|_\rho \frac{\partial^2 u_0}{\partial r^2} \Big|_\rho \right) \cos^2(k\varphi) + 2 \left(u_0|_\rho \frac{\partial u_2}{\partial r} \Big|_\rho + u_2|_\rho \frac{\partial u_0}{\partial r} \Big|_\rho \right) \cos(k\varphi) \\
&\quad + 2u_0|_\rho u_3|_\rho + \frac{\partial u_1^2}{\partial r} \Big|_\rho \cos(k\varphi) + 2u_1|_\rho u_2|_\rho - 2\Delta K_0 \left(\frac{1}{6} \frac{\partial^3 u_0}{\partial r^3} \Big|_\rho \cos^3(k\varphi) \right. \\
&\quad \left. + \frac{1}{2} \frac{\partial^2 u_1}{\partial r^2} \Big|_\rho \cos^2(k\varphi) + \frac{\partial u_2}{\partial r} \Big|_\rho \cos(k\varphi) + u_3|_\rho \right) + 2\Delta^2 (K_0 K_3 + K_1 K_2). \quad (14)
\end{aligned}$$

The solution of the Laplace equation in a ring ($\rho < r < \rho_\lambda$) for each i th system can be written in the form

$$\begin{aligned}
u_i &= A_{0i} + B_{0i} \ln r + \sum_{n=1}^{\infty} r^{-n} (A_{in} \cos(n\varphi) + B_{in} \sin(n\varphi)) \\
&\quad + \sum_{n=1}^{\infty} r^n (E_{in} \cos(n\varphi) + F_{in} \sin(n\varphi)), \quad (15)
\end{aligned}$$

where $i = 0, 1, 2, 3$.

3.1.1. The unperturbed solution (the zeroth order). Substituting (15) with $i = 0$ into (11) and equating the coefficients of the corresponding trigonometric functions, we have

$$A_{0n} = B_{0n} = E_{0n} = F_{0n} = 0, \quad n > 0 \quad (16)$$

$$A_{00} = \Delta - B_{00} \ln \rho_\lambda, \quad (17)$$

$$B_{00} = \frac{\Delta(2A_\lambda(\rho - 1) + \alpha \pm \sqrt{4A_\lambda(\rho - 1)\alpha + \alpha^2})}{2A_\lambda^2 \rho}, \quad (18)$$

where $A_\lambda = \ln(\rho_\lambda/\rho)$.

The concentration field in the solution should satisfy the following two conditions [7–10, 16]:

$$u|_s \rightarrow \begin{cases} \Delta/\rho & \text{if } \alpha \rightarrow 0 \text{ (the diffusion growth regime);} \\ \Delta & \text{if } \alpha \rightarrow \infty \text{ (the kinetic growth regime).} \end{cases} \quad (19)$$

Therefore, the zeroth-order solution can be expressed as

$$u_0 = \Delta + \frac{\Delta(2A_\lambda(\rho - 1) + \alpha - \sqrt{4A_\lambda(\rho - 1)\alpha + \alpha^2})}{2A_\lambda^2\rho} \ln(r/\rho_\lambda). \quad (20)$$

3.1.2. The first-order perturbation solution. As before, substituting (15) with $i = 1$ into the boundary conditions (12) and equating the coefficients of the same trigonometric functions with similar harmonic numbers, we have two first-order nontrivial constants at $n = k$:

$$A_{1k} = A_1 \cdot \rho_\lambda^k, \quad (21)$$

$$E_{1k} = -A_1 \cdot \rho_\lambda^{-k}, \quad (22)$$

where

$$A_1 = \frac{2\Delta^2(\rho - 1)(1 - k^2) + \Delta B_{00}\rho(\alpha - 2(A_\lambda(1 - k^2) - (\rho - 1))) - 2B_{00}^2 A_\lambda \rho^2}{\rho^2(2(z - \frac{1}{z})(\Delta(\rho - 1) - B_{00}\rho A_\lambda) - \alpha k \Delta(z + \frac{1}{z}))}$$

$$z = \rho^k / \rho_\lambda^k.$$

Therefore, the first-order solution to (12) is

$$u_1(r, \varphi) = A_1 \cdot \cos(k\varphi) \left(\frac{\rho_\lambda^k}{r^k} - \frac{r^k}{\rho_\lambda^k} \right). \quad (23)$$

3.1.3. The second-order perturbation solution. In line with the above procedure, we shall substitute (15) with $i = 2$ into the boundary conditions (13). Then the trigonometric function powers are expressed through trigonometric functions of the multiple argument and the coefficients of the same harmonic numbers are equated. This procedure gives four second-order nontrivial constants at $n = 0$ and $n = 2k$:

$$B_{20}, A_{20} = -B_{20} \cdot \ln \rho_\lambda, \quad (24)$$

$$A_{2,2k} = A_2 \cdot \rho_\lambda^{2k}, \quad (25)$$

$$E_{2,2k} = -A_2 \cdot \rho_\lambda^{-2k}, \quad (26)$$

where B_{20} and A_2 are given in the appendix.

Therefore, the second-order solution can be written in the form

$$u_2(r, \varphi) = B_{20} \ln(r/\rho_\lambda) + A_2 \cdot \cos(2k\varphi) \left(\frac{\rho_\lambda^{2k}}{r^{2k}} - \frac{r^{2k}}{\rho_\lambda^{2k}} \right). \quad (27)$$

3.1.4. The third-order perturbation solution. We shall substitute (15) with $i = 3$ into the boundary conditions (14) and, similarly to the second-order procedure, express the trigonometric function powers through trigonometric functions of the multiple argument. Equating the coefficients of the same harmonic numbers, we obtain four nontrivial constants at $n = k$ and $n = 3k$:

$$A_{3,k}, A_{3,3k}, \quad (28)$$

$$E_{3,k} = -A_{3,k} \cdot \rho_\lambda^{-2k}, \quad (28)$$

$$E_{3,3k} = -A_{3,3k} \cdot \rho_\lambda^{-6k}, \quad (29)$$

where $A_{3,k}$ and $A_{3,3k}$, which are expressed through constants of the previous orders, are given in the appendix.

Therefore, $u_3(r, \varphi)$ can be written as

$$u_3(r, \varphi) = \frac{A_{3,k}}{\rho_\lambda^k} \cos(k\varphi) \left(\frac{\rho_\lambda^k}{r^k} - \frac{r^k}{\rho_\lambda^k} \right) + \frac{A_{3,3k}}{\rho_\lambda^{3k}} \cos(3k\varphi) \left(\frac{\rho_\lambda^{3k}}{r^{3k}} - \frac{r^{3k}}{\rho_\lambda^{3k}} \right). \quad (30)$$

Therefore, substituting (20), (23), (27) and (30) into (9), one can write the concentration field $u(r, \varphi)$ as a series in a small parameter δ .

3.2. The critical radius of the morphological stability

The local growth rate V of a crystal to within a positive constant is equal to

$$V \sim \left. \frac{\partial u}{\partial \mathbf{n}} \right|_{r=\rho+\delta \cos(k\varphi)}. \quad (31)$$

We shall substitute $u(r, \varphi)$ into (31) and expand the obtained expression as a series in δ in the neighbourhood of the radius ρ of an unperturbed crystal:

$$V = V_0 + (V_1 \cos(k\varphi) + V_2 \cos(2k\varphi) + V_3 \cos(3k\varphi))/\rho^4, \quad (32)$$

where

$$V_0 = \frac{B_{00}}{\rho} + \frac{(2\frac{A_1}{z}\rho k(z^2+1) + 4B_{02}\rho^2 - B_{00}(k^2-2))\delta^2}{4\rho^3}, \quad (33)$$

$$V_1 = \left(\frac{5}{8} \frac{A_1}{z} \rho k^2 (z^2 - 1) - k^2 \rho^2 \frac{A_2}{z^2} (z^4 - 1) + \frac{A_2}{z^2} \rho^2 k (z^4 + 1) - \frac{3}{4} \frac{A_1}{z} \rho k (z^2 + 1) - A_{3,k} k \rho^{(3-k)} (z^2 + 1) - B_{20} \rho^2 + \frac{3}{8} (k^2 - 2) B_{00} \right) \delta^3 - \left(\frac{A_1}{z} \rho k z^2 + B_{00} + \frac{A_1}{z} \rho k \right) \delta \rho^2, \quad (34)$$

$$V_2 = \rho \left(-\frac{A_1}{z} \rho k^2 (z^2 - 1) - 2 \frac{A_2}{z^2} \rho^2 k (z^4 + 1) + \frac{1}{4} (k^2 + 2) B_{00} + \frac{1}{2} \frac{A_1}{z} \rho k (z^2 + 1) \right) \delta^2, \quad (35)$$

$$V_3 = \left(-\frac{1}{8} (3k^2 + 2) B_{00} - 3A_{3,3k} k \rho^{(3-3k)} (z^6 + 1) - \frac{1}{4} \frac{A_1}{z} \rho k (z^2 + 1) - \frac{1}{2} k^3 \frac{A_1}{z} \rho (z^2 + 1) - 3k^2 \rho^2 \frac{A_2}{z^2} (z^4 - 1) + \frac{A_2}{z^2} \rho^2 k (z^4 + 1) + \frac{7}{8} \frac{A_1}{z} \rho k^2 (z^2 - 1) \right) \delta^3. \quad (36)$$

A traditional method is used to determine the morphological stability radius of a crystal. For this purpose, in line with [4–7], it is necessary to solve the following equation for ρ :

$$V_1 = 0. \quad (37)$$

From (37) it is possible to determine the critical size, after which the variation rate of the initial fundamental harmonic changes its sign from minus (the harmonic decays) to plus (the harmonic grows).

It is seen from (32) that a contribution to this growth rate is made, in addition to the applied perturbing harmonic $\cos(k\varphi)$, by the harmonics $\cos(2k\varphi)$ and $\cos(3k\varphi)$. Therefore, some objections are voiced sometimes [17] as to the use (37) for determination of the morphological

stability radius. Alternatively to this approach, one may analyse the behaviour of two points on the perturbed crystal surface [17]. In this case, the local growth rate is calculated from (32) for two surface points and the conclusion is drawn about stability or instability of the crystal shape depending on whether the points are coming closer or moving apart. However, this method is very subjective since one can take a great number of pairs of points and obtain a number of stable critical radii, which differ not only quantitatively, but also qualitatively [18].

The following is also true of the traditional stability analysis. Higher-order harmonics ($\cos(2k\varphi)$ and $\cos(3k\varphi)$) result from the increase in the fundamental harmonic amplitude $\cos(k\varphi)$ and, therefore, the stability analysis should take into account the growth (decay) rate of this mode only.

The solution to equation (37) is

$$\rho = \rho_0 + \rho_2 \delta^2, \quad (38)$$

where ρ_0 and ρ_2 are expansion coefficients. Since ρ_0 cannot be expressed explicitly, it is numerically determined from the equation $W = 0$ (see W in the appendix). The explicit expression for ρ_2 is not written here because of its awkwardness.

4. Discussion

The linear stability radius ρ_0 and the correction factor of the second order of smallness ρ_2 as a function of α and k are shown in figure 1. According to the calculations (figure 1(a)), the linear stability radius ρ_0 increases with growing perturbation frequency k and the parameter α . This behaviour agrees qualitatively with the behaviour of the linear stability radius ρ_0^* , which was determined earlier in the case of a linear supersaturation dependence of the local growth rate [7]. This behaviour can be explained as follows. It is known [1, 9, 10, 16] that a nonuniform concentration field near the crystal is the primary factor leading to the morphological instability. Indeed, the top of a perturbation, which appears on the crystal surface, is in a more supersaturated solution and, therefore, grows faster than the base of the perturbation (see, specifically, (3)). As a result, the size of the perturbation increases still more. The surface curvature is the main stabilizing factor [1, 9, 10, 16]: the larger the convexity, the more easily the molecules detach from the crystal. For this reason, the increase in the perturbation frequency (when α is fixed) is followed by the growth of the curvature and, correspondingly, the stabilizing factor is enhanced. In other words, in this case the crystal loses its stability at a larger critical size. As α increases, the field near the crystal becomes progressively more uniform, the destabilizing factor decreases and, correspondingly, ρ_0 grows.

It is seen from figure 1(b) that the growth of the perturbation amplitude leads mainly to the decrease in the instability radius as compared to the linear case (the increase is observed only at the harmonic $k = 2$ under the diffusion and intermediate growth regimes). This regularity is also in the qualitative agreement with earlier results [7].

Figures 2(a) and (b) present dependences of the relative differences $(\rho_0^* - \rho_0)/\rho_0$ and $(\rho_2^* - \rho_2)/\rho_2$ on the parameter α at different perturbation frequencies k . Here ρ_2^* is the correction factor of the second order of smallness for the linear supersaturation dependence of the local growth rate [7]. It is seen from these figures that the square-law supersaturation dependence of the growth rate causes the increase in the linear radius, while the correction ρ_2 may be different depending on the growth regime. The ρ_0 value increases because in the case of a nonlinear kinetics of the particle attachment to the surface and a relatively small supersaturation (which is considered in this study) the local growth rate is smaller than in the case of a linear kinetics. Therefore, if the supersaturation is the same, the crystal will remain in the stable state longer in the case of the square-law dependence.

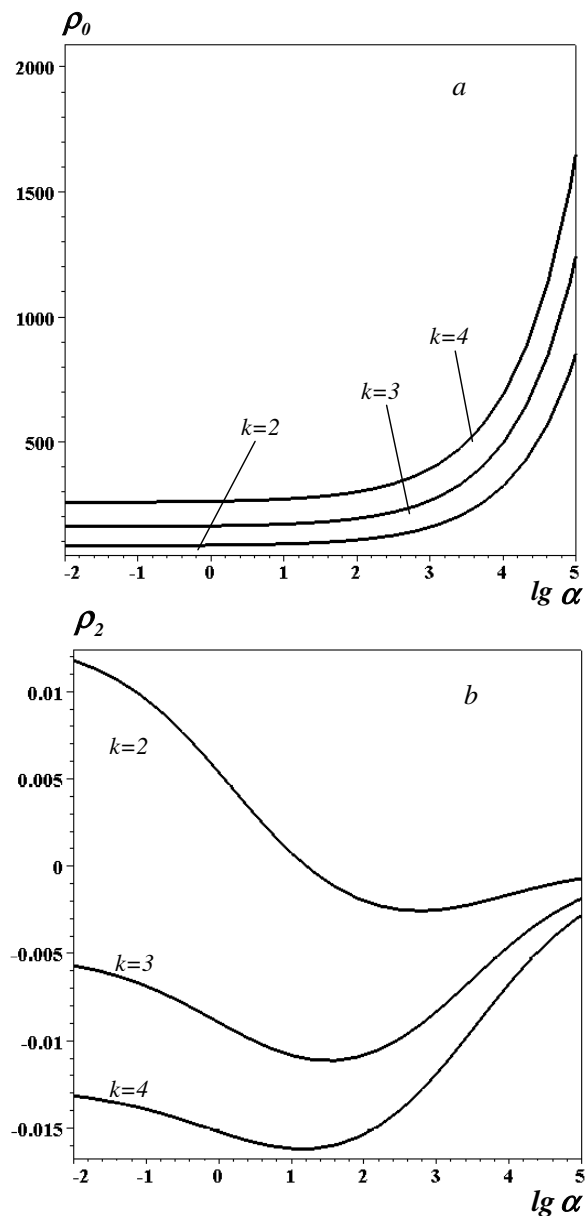


Figure 1. (a) The linear stability radius ρ_0 and (b) the correction factor ρ_2 as functions of the parameter α for different perturbation frequencies k . $\rho_\lambda = 10^8$.

Let us discuss the obtained results in terms of the theory of phase transitions. It was already stated above that the morphological instability of a crystal may be interpreted as a nonequilibrium phase transformation from the initial shape of the crystal to its distorted shape [2, 3]. In this case, ρ_0 may be considered as the spinodal, i.e. the instability point relative to an infinitesimal perturbation [3, 8]. The crystal radius ρ is the stability size in the presence of some finite perturbations. Figure 3 presents the spinodal and the stability radius of a crystal at the perturbation $\delta = \rho_0/4$ depending on the growth regime. It is seen that ρ is virtually

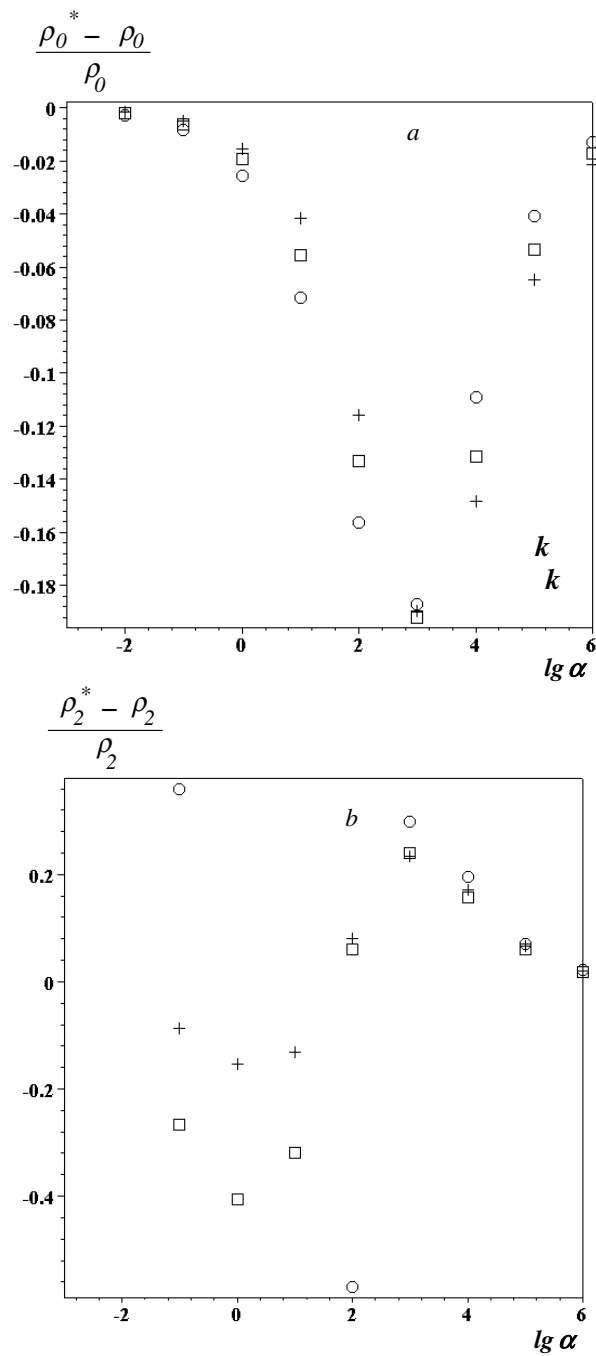


Figure 2. Dependences of (a) the relative difference $(\rho_0^* - \rho_0)/\rho_0$ and (b) the relative difference $(\rho_2^* - \rho_2)/\rho_2$ on the parameter α at different perturbation frequencies k : $k = 2$ (\circ), $k = 3$ (\square), $k = 4$ ($+$). $\rho_\lambda = 10^8$.

always smaller than the corresponding spinodal at every perturbation harmonic. Notice that the spinodal ρ_0 at the harmonic k crosses ρ at $k + 1$ for the intermediate and kinetic growth of

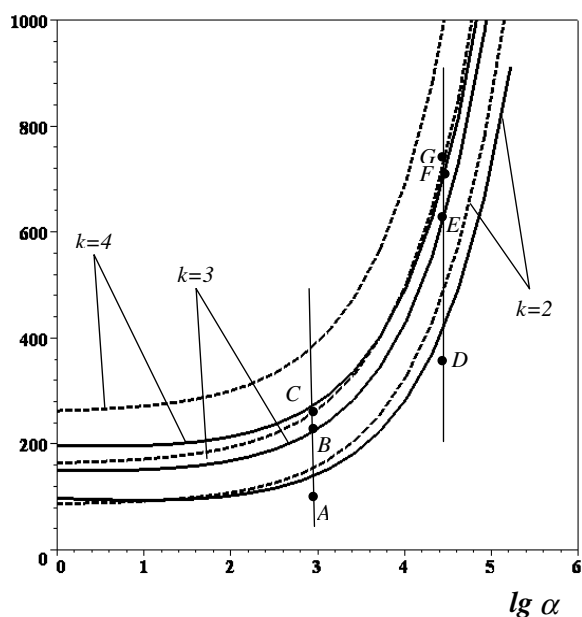


Figure 3. Critical sizes ρ_0 (dashed curve) and ρ (solid curve) (at the perturbation $\delta = \rho_0/4$) depending on the parameter α and k .

the crystal (α is large). As a result, in terms of the adopted formalism, various nonequilibrium morphological phases may coexist if perturbations of different frequencies and amplitudes are present in the solution. We shall give two examples (see figure 3). Let a solution contain perturbations having only two frequencies $k = 3$ and 4 and amplitudes not larger than $\rho_0/4$.

The first case: several crystals grow from a solution and $lg \alpha = 3$. Their evolution is described by the straight line AC (figure 3). According to the calculations, the crystal growth will be stable up to the point B and the crystals will be round. Starting from the point B some crystals at localization sites of perturbations will become unstable relative to perturbations with $k = 3$, while the other crystals will continue their stable growth. Therefore, crystals having two shapes—a round shape and like the one shown in figure 4(a)—will be observed over the interval BC. Starting from the point C (the spinodal point for perturbations with $k = 3$) the initial round shape of the crystals will be unstable relative to perturbations with any infinitely small amplitude and $k = 3$. Therefore, the probability that a crystal having the initial round shape occurs after the point C becomes negligibly small and, consequently, all the observed crystals will be of the type shown in figure 4(a).

The second case: several crystals grow from a solution and $lg \alpha = 4.5$. In line with the reasoning adduced in the first case, we may come to the following result. Only initially round crystals grow over the interval DE. Both round crystals and crystals like those in figure 4(a) can grow over the interval EF. Crystals of three types—round crystals and those like in figures 4(a) and (b)—can grow simultaneously starting from the point F and ending with the point G (the spinodal for perturbations with $k = 3$). After the point G all remaining round crystals will be unstable relative to perturbations with $k = 3$.

Notice also that crystals should not necessarily pass all possible stages during their growth both in the first and second cases. Specifically, crystallization conditions may change rather quickly and crystals will stop growing and preserve the shape characteristic of a particular stage of their growth.

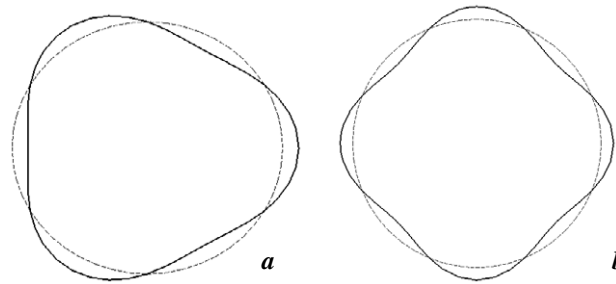


Figure 4. The shape of crystals when the third, $k = 3$ (a), and fourth, $k = 4$ (b), harmonics grow.

So, the obtained results imply the simultaneous growth of crystals having different shapes under the same nonequilibrium growth conditions. This inference was verified qualitatively in experiments [12–14]. It should be noted that the intersection of metastable regions (these are areas between ρ and ρ_0 for different k) was also determined analytically using an absolutely different approach (calculations of the entropy production in a crystallizing system) [3, 8, 15].

5. Conclusion

A weakly nonlinear analysis of the morphological stability of a round crystal was performed for the first time to the third order of the perturbation theory assuming an arbitrary growth regime and a square-law dependence of the local growth rate on the supersaturation. It was found that the crystal stability radius decreased with increasing amplitude of the perturbation harmonics higher than the second harmonic under all conditions. This observation explained the phenomenon of the coexistence of morphological phases. The obtained results were compared with the data obtained earlier for a linear dependence of the local growth rate on the supersaturation. They were found to be qualitatively similar. Quantitative differences were analysed.

Although the deduced formulae proved to be relatively cumbersome, they seem to be useful for practical purposes and provide a real opportunity of comparison with experiments. The most interesting issue in the future will be measurements of the critical crystal stability size at different amplitudes and frequencies of perturbations in various growth regimes (from diffusion to kinetic conditions). Such experiments will provide both a more rigorous verification of the classical theory of the morphological stability and a more careful examination of the analogy between classical and nonequilibrium phase transitions.

Appendix

$$K_0 = \frac{1}{\rho};$$

$$K_1 = \frac{(k^2 - 1) \cos k\varphi}{\rho^2};$$

$$K_2 = \frac{1}{\rho^3} \left[\frac{k^2}{2} + \left(1 - \frac{5}{2}k^2 \right) \cos^2 k\varphi \right];$$

$$K_3 = \frac{1}{\rho^4} \left[\left(\frac{3}{2}k^4 + \frac{9}{2}k^2 - 1 \right) \cos^3 k\varphi - \frac{3}{2}k^2(1 + k^2) \cos k\varphi \right].$$

$$B_{20} = \frac{1}{4} \{ \rho^3 [2A_\lambda \rho (\Delta - B_{00} A_\lambda) + (\alpha - 2A_\lambda) \Delta] \}^{-1} \left\{ s\rho^4 + f\rho^3 \right. \\ \left. + 2\rho^2 \left[\left(A_1 k \left(z + \frac{1}{z} \right) (2 - \alpha) + 2A_1 \left(z - \frac{1}{z} \right) (k^2 - 1) - B_{00} \right) \Delta \right] \right\}$$

$$\begin{aligned}
& + (1 + A_\lambda) B_{00}^2 \Big] + \Delta \rho [2(\Delta - B_{00} A_\lambda)(3k^2 - 2) \\
& + B_{00}(\alpha(k^2 - 2) + 2(3 - 2k^2))] + 2\Delta^2(k^4 - 5k^2 + 3) \Big\}; \\
A_2 = & \frac{1}{8} \left\{ \rho^3 \left[\left(z^2 - \frac{1}{z^2} \right) (\rho \Delta - \rho A_\lambda B_{00} - \Delta) - \Delta \alpha k \left(z^2 + \frac{1}{z^2} \right) \right] \right\}^{-1} \left\{ s \rho^4 + f \rho^3 \right. \\
& + 2\rho^2 \left[\left(k A_1 \left(z + \frac{1}{z} \right) (2 - \alpha) + A_1 \left(z - \frac{1}{z} \right) (2k^2 \alpha + 2k^2 - 2) - B_{00} \right) \Delta \right. \\
& + (1 + A_\lambda) B_{00}^2 \Big] + \Delta \rho [(10k^2 - 4)(\Delta - B_{00} A_\lambda) - B_{00} \alpha (k^2 + 2) \\
& \left. \left. - 2B_{00} (2k^2 - 3)] + 2\Delta^2 (k^4 - 7k^2 + 3) \right\}
\end{aligned}$$

where

$$\begin{aligned}
s = & 2A_1^2 \left(\frac{1}{z^2} + z^2 - 2 \right); \quad f = 4A_1 \left[k \left(z + \frac{1}{z} \right) (B_{00} A_\lambda - \Delta) - \left(z - \frac{1}{z} \right) B_{00} \right] \\
A_{3,k} = & -\frac{1}{8} \left\{ \rho^4 \left(\Delta \alpha k \left(z + \frac{1}{z} \right) + 2(A_\lambda \rho B_{00} - \Delta \rho + \Delta) \left(z - \frac{1}{z} \right) \right) \right\}^{-1} \\
& \times \left\{ \rho^5 \left[2A_1 B_{00} A_\lambda \left(z - \frac{1}{z} \right) + A_1 A_2 \left(\left(z^3 + \frac{1}{z^3} \right) - \left(z + \frac{1}{z} \right) \right) \right] \right. \\
& + 4\rho^4 \left[4A_2 \left(z^2 + \frac{1}{z^2} \right) (B_{00} - \Delta k) + \left(z^2 - \frac{1}{z^2} \right) (3k A_1^2 - 2B_{00} A_2) \right. \\
& \left. - 4B_{20} (\Delta - 2A_\lambda B_{00}) \right] + \rho^3 \left[\Delta \left(8B_{20} (2A_\lambda (k^2 - 1) + \alpha - 2) \right. \right. \\
& \left. \left. + 8A_2 \left(\left(z^2 - \frac{1}{z^2} \right) (\alpha k^2 + k^2 - 1) + \left(z^2 + \frac{1}{z^2} \right) (2k - \alpha k) \right) \right. \right. \\
& \left. \left. + 6A_1 k \left(\left(z + \frac{1}{z} \right) - k \left(z - \frac{1}{z} \right) \right) \right) + 6A_1 B_{00} \left(\left(z - \frac{1}{z} \right) A_\lambda k^2 \right. \right. \\
& \left. \left. + 1 - k \left(z + \frac{1}{z} \right) (A_\lambda - 2) \right) \right] + \rho^2 \left[A_1 \Delta \alpha k \left(6 \left(z + \frac{1}{z} \right) - 5k \left(z - \frac{1}{z} \right) \right) \right. \\
& \left. + 2\Delta \left(2B_{00} + A_1 \left(3k \left(z + \frac{1}{z} \right) (2k^2 - 3) - 2 \left(z - \frac{1}{z} \right) (4k^2 - 3) \right) \right) \right. \\
& \left. - 2B_{00}^2 (2A_\lambda + 3) \right] + \Delta \rho \left[\Delta (6k^4 - 30k^2 + 12) \right. \\
& \left. - (6A_\lambda k^4 - 30A_\lambda k^2 + 3\alpha k^2 - 28k^2 + 12A_\lambda - 6\alpha + 22) B_{00} \right] \\
& \left. - \Delta^2 (28k^4 - 64k^2 + 24) \right\} \rho_\lambda^k \\
A_{3,3k} = & \frac{1}{24} \left\{ \rho^4 \left(2\rho \left(z^3 - \frac{1}{z^3} \right) (\Delta - A_\lambda B_{00}) - 3\Delta \alpha k \left(z^3 + \frac{1}{z^3} \right) - 2\Delta \left(z^3 - \frac{1}{z^3} \right) \right) \right\}^{-1} \\
& \times \left\{ 24\rho^5 A_1 A_2 \left(\left(z^3 + \frac{1}{z^3} \right) - \left(z + \frac{1}{z} \right) \right) \right. \\
& \left. + \rho^4 \left[12 \left(z^2 - \frac{1}{z^2} \right) (A_1^2 k - 2A_2 B_{00}) + 48A_2 k \left(z^2 + \frac{1}{z^2} \right) (B_{00} A_\lambda - \Delta) \right] \right\}
\end{aligned}$$

$$\begin{aligned}
& + \rho^3 \left[6A_1 \left(B_{00} \left(z - \frac{1}{z} \right) (A_\lambda k^2 + 2k + 1) - A_\lambda k \left(z + \frac{1}{z} \right) \right. \right. \\
& + \Delta k \left(z + \frac{1}{z} \right) - k \left(z - \frac{1}{z} \right) \left. \left. + 24A_2 \Delta \left(\left(z^2 + \frac{1}{z^2} \right) (2k - \alpha k) \right. \right. \right. \\
& + \left. \left. \left(z^2 - \frac{1}{z^2} \right) (k^2 + 3\alpha k^2 - 1) \right) \right] \\
& + \rho^2 \left[4\Delta B_{00} - 2B_{00}^2 (2A_\lambda + 3) + A_1 3\Delta \left(z - \frac{1}{z} \right) \right. \\
& \times (4 - 6k - 7\alpha k^2 - 8k^2) + 6\Delta k A_1 \left(z + \frac{1}{z} \right) (\alpha + 2\alpha k^2 + 2k^2) \left. \right] \\
& + \rho \left[B_{00} \Delta A_\lambda (18k^4 + 54k^2 - 12) + \Delta^2 (12 - 54k^2 - 18k^4) \right. \\
& + \left. B_{00} \Delta (36k^2 - 22 + 6\alpha + 9\alpha k^2) + 12\Delta^2 (-k^4 + 8k^2 - 2) \right] \rho_\lambda^{3k} \\
W = & \Delta \sqrt{4A_\lambda \rho_0 \alpha - 4A_\lambda \alpha + \alpha^2} \left\{ 2\rho_0^4 A_\lambda^2 \left(\left(h - \frac{1}{h} \right) + k \left(h + \frac{1}{h} \right) \right) \right. \\
& + 2\rho_0^3 A_\lambda \left(k \left(h + \frac{1}{h} \right) (A_\lambda^2 (1 - k^2) - A_\lambda + \alpha) + \left(h - \frac{1}{h} \right) (\alpha - A_\lambda) \right) \left. \right\} \\
& - \Delta \left\{ 6\rho_0^4 A_\lambda^2 \alpha \left(\left(h - \frac{1}{h} \right) - k \left(h + \frac{1}{h} \right) \right) - 2A_\lambda \alpha \rho_0^3 \left[A_\lambda \left(h - \frac{1}{h} \right) (3 - \alpha) \right. \right. \\
& + \left. \left. k (3A_\lambda - \alpha + A_\lambda^2 (k^2 - 1)) \right] \right\}
\end{aligned}$$

where $h = \frac{\rho_0^k}{\rho_\lambda^k}$.

References

- [1] Coriell S R and McFadden G B 1993 *Handbook of Crystal Growth* vol 1, part B, ed D T J Hurlle (Amsterdam: North-Holland)
- [2] Ben-Jacob E and Garik P 1990 *Nature* **343** 523–30
- [3] Martyushev L M, Seleznev V D and Kuznetsova I E 2000 *JETP* **91** 132–43
- [4] Brush L N, Sekerka R F and McFadden G B 1990 *J. Cryst. Growth* **100** 89–108
- [5] Debroy P P and Sekerka R F 1995 *Phys. Rev. E* **51** 4608–20
- [6] Debroy P P and Sekerka R F 1996 *Phys. Rev. E* **53** 6244–52
- [7] Martyushev L M, Sal'nikova E M and Chervontseva E A 2004 *JETP* **98** 986–96
- [8] Martyushev L M and Sal'nikova E M 2003 *J. Phys.: Condens. Matter* **15** 1137–46
- [9] Chernov A A 1971 *Sov. Phys.—Crystallogr.* **16** 734–54
- [10] Chernov A A 1984 *Modern Crystallography* vol III (Berlin: Springer)
- [11] Ovsienko D E, Alifintsev G A and Maslov V V 1974 *J. Cryst. Growth* **26** 233–8
- [12] Shibkov A A *et al* 2001 *Crystallogr. Rep.* **46** 496–503
- [13] Shochet O and Ben-Jacob E 1993 *Phys. Rev. E* **48** 4168–72
- [14] Sawada Y *et al* 1991 *Phys. Rev. A* **43** 5537–41
- [15] Martyushev L M, Kuznetsova I E and Nazarova A S 2004 *Phys. Solid State* **46** 2115–20
- [16] Coriell S R and Parker R L 1965 *J. Appl. Phys.* **36** 632–7
- [17] Seleznev V D 2003 private communication
- [18] Chervontseva E A 2004 *MS Thesis* Molecular Physics Department, Ural State Technical University